Pharm Res (2012) 29:2754–2765
DOI 10.1007/s11095-012-0689-5

RESEARCH PAPER

Molecular Weight Effects on the Miscibility Behavior of Dextran and Maltodextrin with Poly(vinylpyrrolidone)

Bernard Van Eerdenbrugh • Lynne S. Taylor

Received: 7 October 2011 / Accepted: 17 January 2012 / Published online: 2 February 2012

ABSTRACT

Purpose To characterize and interpret the miscibility of dextran and maltodextrin with poly(vinylpyrrolidone) (DEX-PVP) as a function of polymer molecular weights.

Methods Blend miscibility was studied using 4 different molecular weight (MW) grades of DEX combined with 5 MW grades of PVP, over a broad compositional range. Miscibility was evaluated by inspection of glass transition events measured by differential scanning calorimetry (DSC). Fourier transform mid-infrared spectroscopy (FTIR), combined with curve fitting, was performed to characterize the extent of hydrogen bonding. The observed miscibility behavior was further interpreted in terms of mixing thermodynamics.

Results Miscibility of the blends ranged from fully miscible to completely immiscible with multiple partially miscible systems observed. Increasing polymer molecular weight decreased miscibility. For the lowest DEX grade, hydrogen bonding was independent of PVP MW, as expected since all systems were completely miscible. Higher molecular weights of DEX resulted in reduced intermolecular hydrogen bonding and decreased miscibility, increasingly so for higher MW PVP grades. Evaluation of the mixing thermodynamics supported these findings.

Conclusions With higher combined molecular weights of DEX-PVP blends, phase behavior evolves from completely miscible to virtually immiscible. Concurrently, DEX-PVP hydrogen bonding decreases. From a thermodynamic perspective, the combinatorial mixing entropy was observed to decrease as the molecular weight of the polymers increased, providing a reduced counterbalance to the unfavorable mixing enthalpy thought to accompany this polymer combination.

KEY WORDS dextran · differential scanning calorimetry (DSC) · maltodextrin · mid infrared spectroscopy · miscibility · molecular weight · phase separation · poly(vinylpyrrolidone)

INTRODUCTION

The characterization of miscibility in amorphous pharmaceutical systems is a topic of historical and current interest. Examples of systems where miscibility plays an important role in drug product performance include amorphous solid dispersions and freeze-dried formulations. In the former case, an amorphous drug is intimately mixed with a polymeric carrier (1), and attaining miscibility is considered favorable in the sense that it increases the likelihood of conserving the amorphous form of the drug for prolonged periods of time, compared to the amorphous form without polymer (2,3). Indeed, it has been reasoned and can be intuitively understood that in phase-separated systems, the drug will be more prone to crystallization as there is less polymer available for physical stabilization of the drug-rich phase (4). For freeze-dried formulations, polymers and/or small molecules are added to protect the active ingredient (e.g. a protein) against deleterious chemical and physical changes during the freezing, drying and storage steps, as well as to facilitate the formation of a glassy solid with a glass transition temperature (T_g) higher than the intended storage temperature (5).

Electronic supplementary material The online version of this article (doi:10.1007/s11095-012-0689-5) contains supplementary material, which is available to authorized users.

B. Van Eerdenbrugh · L. S. Taylor (✉)
Department of Industrial and Physical Pharmacy, College of Pharmacy
Purdue University
575 Stadium Mall Drive
West Lafayette, Indiana 47907, USA
e-mail: lstaylor@purdue.edu

B. Van Eerdenbrugh
Laboratory for Pharmacotechnology and Biopharmacy
K.U. Leuven, Gasthuisberg O&N2
Herestraat 49, box 921
3000 Leuven
Belgium

Traditionally, differential scanning calorimetry (DSC) has been the most extensively used characterization technique applied for miscibility evaluation (4). Where a single glass transition (T_g) event is expected for a miscible system, evidence of phase separation is inferred from the observation of two T_g events (4). However, a number of issues are known to be associated with this methodology (4); potential problems include (i) the difficulty of resolving T_g events of mixture components having similar T_g values, (ii) limitations in terms of minimal domain sizes needed to enable the detection of phase-separated domains (e.g. 10–50 nm for polymeric blends) (6,7), and (iii) glass transition regions of materials can sometimes be broad and/or have small changes in heat capacity, challenging the capability of the technique to identify T_g events (see Baird and Taylor for a more detailed discussion) (4). Furthermore, the fact that the determination of glass transition events by DSC involves heating of the sample through the glass transition temperature region(s) of the sample, may have an effect on miscibility which varies with temperature.

Therefore, the implementation of complementary techniques and the development of new methodologies for miscibility evaluation is an important area of research. Potential alternative techniques that have been explored to some extent include Fourier transform mid-infrared spectroscopy (FTIR, with or without further multivariate analysis) (8–10), X-ray powder diffraction (XRPD, with or without subsequent calculation of pair distribution functions) (7,10–12), solid state nuclear magnetic resonance (SSNMR) (13–15), atomic force microscopy (AFM) (9,16), scanning and/or transmission electron microscopy (SEM/TEM) (9,13), Raman mapping (12,17,18), local (photo)thermal analysis (19–22) and nanoscale infrared spectroscopy (23,24).

Several studies exploring the miscibility of dextran-PVP (DEX-PVP) blends have been reported (e.g. 7,12,25–28). A number of these describe the miscibility of DEX-PVP systems in freeze-concentrated solutions in the presence or absence of additives (25–27). Other studies evaluate the miscibility of DEX-PVP systems in the solid state (7,12,28). In one study (28), the miscibility of high molecular weight blends of DEX (molecular weight 520 kDa) and PVP (PVP K 90, molecular weight 1,000 kDa) was evaluated using DSC, and complete immiscibility was observed. In another investigation, X-ray powder diffraction was used to evaluate miscibility in a blend of high MW grades of both polymers (DEX of 64–76 kDa and PVP K 90) (7), and the authors concluded that the system was completely immiscible. In a more recent study (12), DSC, Raman mapping and XRPD analysis were used to evaluate the miscibility of two DEX-PVP systems, one combining polymers of relatively high molecular weights (DEX of 8.5–11.5 kDa with PVP of 29 kDa) and another combination with relatively low polymer molecular weights (DEX of 4-6 kDa and PVP of 10 kDa). Again, phase separation appeared to be the dominant process across all compositions. Hence, in systems where the miscibility of DEX-PVP systems has been evaluated in the solid state, relatively high polymer molecular weights have been studied leading to largely immiscible systems. In one study, however, the miscibility of a very closely related polymer system (29) was investigated. Here, the miscibility of PVP was evaluated with maltodextrin and it was found that miscible blends were obtained upon freeze-drying PVP K 90 with maltodextrins (molecular weights of 860 and 1,050 Da). Based on the molecular structures of the polymers (Fig. 1), it can be seen that maltodextrin and dextran have similar chemical structures. Both polymers

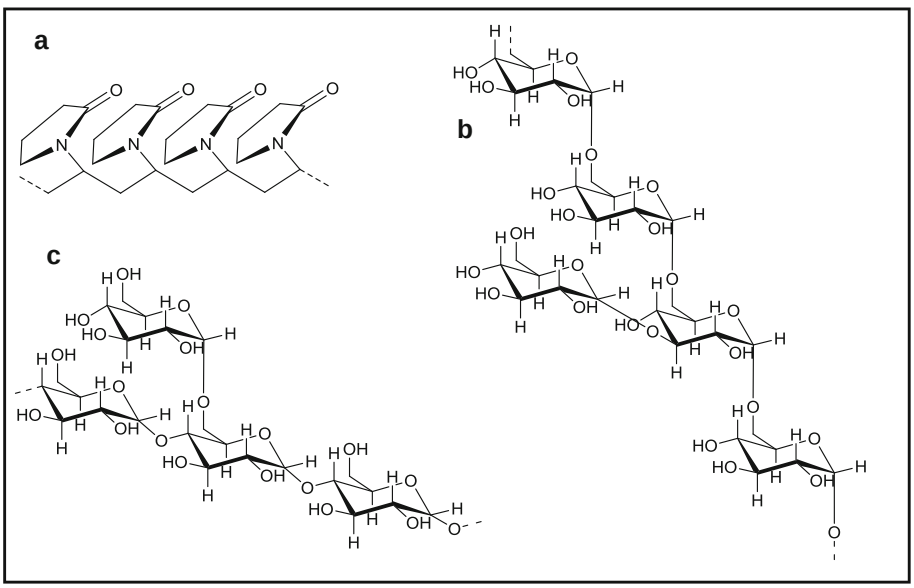

Fig. 1 Molecular structures of the different polymers used in this study: (**a**) PVP, (**b**) dextran, and (**c**) maltodextrin.

are composed of D-glucose units. While dextrans consist of a backbone where the glucose units are 1-6 linked with a low degree (approximately 5 %) of branched, short (mostly 1 or 2 glucose units) 1-3-linked sidechains, maltodextrins can be considered as low molecular weight analogues where the glucose units of the backbone are linked by 1-4 bonds, with 1,6 connected branches. Given the excellent chemical similarity between dextrans and maltodextrin, maltodextrins will be applied as low MW analogs of dextrans and the term DEX will refer to both dextran and maltodextrin in the remainder of this report.

DEX-PVP systems have a number of features that make them interesting model systems for the evaluation of novel characterization approaches to study miscibility. First, both polymers are amorphous, resulting in the formation of fully amorphous blends upon mixing. As crystallization cannot occur in these systems, the interpretation of results can be limited to the differentiation between amorphous-amorphous phase separation and the formation of miscible blends. Second, it is well known that polymer molecular weight is a key factor that influences miscibility (30). Thus, by changing molecular weights of the polymers, systems with variable miscibility characteristics but virtually constant chemical composition potentially can be obtained. Ideally, demonstrating the ability of an analytical technique to characterize miscibility should involve testing of miscible, partially miscible and immiscible systems of the same constituents, thereby eliminating chemical variation.

In this work, a comprehensive study of the miscibility behavior of blends of dextran or maltodextrin (DEX) in combination with PVP as a function of composition and polymer molecular weight is reported. Structures of the polymers are provided in Fig. 1 and key characteristics of the various grades used can be found in Table I. Miscibility was evaluated using DSC and FTIR spectroscopy. Further analysis of the FTIR spectra was performed using curve fitting to evaluate the extent of intermolecular hydrogen bonding in the mixtures. Finally, mixing thermodynamics were considered to further rationalize the miscibility trends observed.

Table I Overview of the Different Grades of the Polymers Used in this Study, their Corresponding Molecular Weights and the Abbreviations Used

Polymer and grade	Abbreviation	Molecular weight (Da)[a]
Poly(vinylpyrrolidone) – K 12	PVP12	2,000–3,000
Poly(vinylpyrrolidone) – K 17	PVP17	7,000–11,000
Poly(vinylpyrrolidone) – K 25	PVP25	28,000–34,000
Poly(vinylpyrrolidone) – K 30	PVP30	44,000–54,000
Poly(vinylpyrrolidone) – K 90	PVP90	1,000,000–1,500,000
Maltodextrin	DEX1	783
Dextran – low MW	DEX6	6,000
Dextran – medium MW	DEX40	40,000
Dextran – high MW	DEX450	400,000–500,000

[a] As obtained from the manufacturer

MATERIALS AND METHODS

Materials

Polyvinylpyrrolidones [PVP, Kollidon®, K 12 (PVP12), K 17 (PVP17), K 25 (PVP25), K 30 (PVP30), K 90 (PVP90)] were kindly provided by BASF Aktiengesellschaft (Ludwigshafen, Germany). Dextrans [from *Leuconostoc* spp., molecular weights 6,000 (DEX6), 40,000 (DEX40), 400,000–500,000 (DEX450)] were purchased from Sigma-Aldrich Co. (St. Louis, MO, USA). Maltodextrin (extra low MW grade, molecular weight 783 g/mol (DEX1)] was obtained from V-LABS Inc, Covington, LA, USA).

Preparation of Dextran-PVP Solutions

Aqueous DEX-PVP solutions [10 % (w/v) total solids] were prepared in different weight ratios [10/90, 20/80, 30/70, 40/60, 50/50, 60/40, 70/30, 80/20 and 90/10 (w/w) DEX-PVP] by mixing the pure solutions [0/100 and 100/0 (w/w) DEX-PVP] in volume ratios, identical to the resulting weight ratios. Samples were stored in a refrigerator prior to further use.

Differential Scanning Calorimetry

Glass transition temperatures (T_g) of the samples were determined using a TA Q2000 DSC equipped with a refrigerated cooling accessory (TA Instruments, New Castle, DE, USA). For the preparation of the bulk samples, solutions of DEX and/or PVP were freeze-dried in 2 ml vials (Wheaton Science Products, Millville, NJ, USA). After filling the vials, rubber stoppers (Wheaton Science Products, Millville, NJ, USA) were gently placed on top of the vials so that contact between the vial interior and the sample chamber was maintained and lyophilization was performed using a programmable bench top lyophilizer (VirTis, Gardner, NY, USA) and a fixed lyophilization cycle (Table II). After completion of the cycle, the vials were closed, the lyophilizer was brought to atmospheric pressure and vials were removed from the instrument. Vials were then stored under vacuum overnight, to further remove residual water. Samples, prepared in aluminum pans with a pin hole, were heated to either 200 °C (for samples containing DEX1) or 250 °C (all other samples) using a heating rate of 10 °C/min. Subsequently, samples were held isothermally for 1 min, cooled to 40 °C using a cooling rate of 10 °C/min, held isothermally for 1 min followed by reheating the sample using a heating rate of 10 °C/min. From

Table II Overview of the Lyophilization Cycle Used for Freeze-Drying the Dextran-PVP Samples

	Freezing step		Primary drying				Secondary Drying
Step	1	2	3	4	5	6	7
Temperature (°C)	−2	−40	−35	−20	−5	5	20
Duration (h)	0.5	1	10	10	5	5	5
Total time (h)	0.5	1.5	11.5	21.5	26.5	31.5	36.5
Vacuum (mTorr)	N/A	N/A	100	100	100	100	150

N/A not applicable

the resulting thermograms, T_g events were determined as the midpoint of the glass transition events observed in the second heating run, except for samples containing DEX1, where the analysis was performed on the first heating run of the samples, as degradation was often observed at higher temperatures for these samples.

Fourier Transform Mid-Infrared Spectroscopy

For collection of Fourier transform mid-infrared (FTIR) transmission spectra, DEX-PVP solutions were spin-coated onto KRS-5 substrates. A few drops of the solution was placed on the substrate, and rotated using a KW-4A spin-coater (Chemat Technology Inc., Northridge, CA, USA) at 8,000 rpm for 20 s. Subsequently, the thin films were stored overnight under a dry nitrogen purge (<10 % relative humidity), to remove residual water. Spectra of the resulting thin films were obtained in transmission mode using a Bio-Rad FTS 6,000 spectrophotometer (Bio-Rad Laboratories, Hercules, CA, USA) equipped with globar infrared source, KBr beamsplitter, and DTGS detector. The scan range was set from 500 to 4000 cm^{-1} with 4 cm^{-1} resolution, and 128 scans were co-added. During infrared measurements, the spin-coated samples and the sample compartment of the spectrophotometer were flushed with dry air (<10 % relative humidity) in order to further minimize interference from absorbed and gas-phase moisture. Spectra were recorded for 0/100, 20/80, 50/50, 80/20 and 100/0 (w/w) DEX-PVP mixtures for all DEX and PVP grades. In addition, spectra were collected for all DEX-PVP ratios prepared for the DEX1-PVP12 system. Background corrections were performed on all samples. For further determination of the extent of hydrogen bonding based on changes in the PVP carbonyl stretching peak, the latter was corrected for the contribution of the peak of DEX1 at 1600 cm^{-1}, by subtracting the spectrum of the pure DEX1 from those of the DEX1-PVP blends using an appropriate factor. This was not necessary for samples containing other DEX grades, as the contribution of that peak was negligible in these samples. All PVP peaks were normalized to the area under the curve. Subsequently, spectra of the DEX-PVP blends were fitted to the spectra of non-hydrogen bonded PVP (the pure PVP spectrum) and that of the maximally hydrogen bonded PVP carbonyl peak [using the 0.9 (w/w) DEX weight fraction of the DEX1-PVP12 system], keeping the sum of the factors by which the spectra were multiplied equal to 1. The optimal fit was obtained by minimizing the sum of the squares of the residuals over the 1590–1750 cm^{-1} spectral range. The latter was expressed as a percentage, relative to the spectral data (by taking the ratio of the square root of the sum of squares and the sum of the intensities in the spectral data). Additional detail on the determination of the degree of hydrogen bonding can be found in the Discussion section.

RESULTS

Very Low MW Dextran Analog (DEX1) with Different PVP Grades

For DEX1 systems, representative DSC and FTIR data are provided in Fig. 2a and b, respectively. DSC data of the DEX1-PVP25 system (Fig. 2a) shows a single T_g event for all compositions whereby the T_g increases with an increasing amount of the higher T_g component (PVP25). These results suggest the formation of a miscible system over the complete composition range (4). Similar phase behavior was observed for all other PVP grades in combination with DEX1 (see Figure S1 in the Supplementary Material). Hence based on DSC data, PVP is miscible with DEX1 for all the MW grades evaluated and over the complete compositional range. FTIR data of the carbonyl stretching band of PVP in DEX1-PVP12 blends are provided in Fig. 2b. This band has been described as a mixed mode containing combinations from carbonyl stretching and N-C stretching vibrations (31–33). Since the carbonyl function has hydrogen bond acceptor character and PVP lacks hydrogen bond donors, it forms a useful probe to assess intermolecular hydrogen bonding with a hydrogen bond donor (29,33). In contrast, DEX has the ability to undergo hydrogen bonding with itself, both intermolecularly and intramolecularly. The formation of homo and hetero (with PVP) hydrogen bonds would be expected to influence the DEX

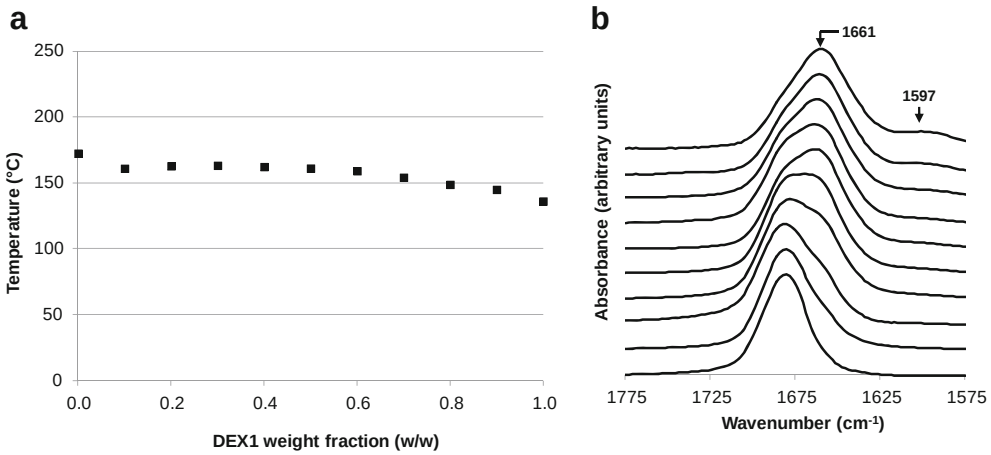

Fig. 2 Representative DSC and FTIR results for DEX1-based systems: (**a**) variation of the T_g as a function of the DEX weight fraction for the DEX1-PVP25 system, and (**b**) changes in the PVP carbonyl stretching peak as a function of the DEX weight fraction for the DEX1-PVP12 system (normalized and offset). Key: from bottom to top: 0, 0.1, 0.2, 0.3, 0.4, 0.5, 0.6, 0.7, 0.8 and 0.9 (w/w) DEX weight fraction.

O-H stretching bands whereby the formation of hydrogen bonds with PVP would occur at the expense DEX-DEX interactions. As a result, interpretation of spectral changes in the O-H stretching bands is more complicated than interpretation of changes to the PVP carbonyl stretching band and has therefore not been further considered to the same extent that changes in the PVP carbonyl band were investigated. For pure PVP [Fig. 2b, 0 (w/w) DEX weight fraction] the maximum of the (non-hydrogen bonded) carbonyl stretching band lies at 1680 cm^{-1}. Upon mixing PVP12 with DEX1, a second lower wavenumber band gradually develops, showing a maximum at 1661 cm^{-1}. This red-shifted band corresponds to the hydrogen bonded carbonyl group, as the weakening of the energy of the carbonyl vibration due to hydrogen bonding causes the band to shift to lower wavenumbers. This extensive hydrogen bonding between DEX1 and PVP12 is in excellent agreement with the proposed miscibility suggested from the DSC results. For high dilutions of PVP12 [0.8 and 0.9 (w/w) DEX fraction], two observations can be made: First, the carbonyl peak remains virtually unchanged. This suggests that at these dilutions, hydrogen bonding with DEX is maximal. It is important to note that this state of maximum hydrogen bonding of carbonyl groups does not necessarily mean that all PVP carbonyl groups participate in hydrogen bonding. Previous observations showed that hydrogen bonding interactions between PVP and maltodextrin were lower than those observed between e.g. sucrose and PVP, which was interpreted as being due to differences in the extent of hydrogen bonding and not caused by alterations in the strength of the hydrogen bonds (29). This agrees well with observations made in other polymer systems, where it was suggested that factors such as steric constraints may explain the observation that even at high dilutions, a non-hydrogen bonding fraction still remains (34). Second, for these samples with high DEX1 fractions, an additional weak band develops [maximum at 1597 cm^{-1} for the 0.9 (w/w) DEX fraction sample]. This band which originates from DEX1 lies at 1601 cm^{-1} in the pure sample (data not shown). FTIR results on the other PVP grades mixed with DEX1 are very similar to those obtained from the DEX1-PVP12 (see Figure S2 in the Supplementary Material). Hence, DEX1-based systems are miscible over their whole composition range and extensive hydrogen bonding occurs between PVP carbonyl groups and DEX1 hydroxyl groups.

Low MW Dextran (DEX6) with Different PVP Grades

On moving to a higher molecular weight dextran grade (DEX6), the miscibility behavior of the systems starts to change. As can be seen from the DSC data for the DEX6-PVP25 system (Fig. 3a), the system ceases to be miscible over the whole composition range whereby two T_g events can be observed for DEX weight fractions between 0.5 and 0.8 (w/w) indicating the development of a miscibility gap (i.e. a region of immiscibility can be observed) (4). Based on the T_g values of the pure polymers, for compositions where two T_g events are observed, the lower T_g values correspond to the PVP-rich phase, while the higher T_g values correspond to the DEX-rich phase. Similar behavior can be seen for the DEX6-PVP30 and DEX6-PVP90 systems (see Figure S3 in the Supplementary Material). For the lower molecular weight PVP grades, the miscibility gap tends to become smaller (DEX6-PVP17) or disappear entirely (DEX6-PVP12) (see Figure S3 in the Supplementary Material). In addition, it can be noted that (i) the miscibility gap, i.e. the compositional region where phase separation is observed, tends to occur at high DEX weight fractions, and (ii) where phase separation is observed, the T_g values of the PVP-rich phase tend to vary with composition while the T_g values of the DEX-rich phase are more uniform and close to the values seen for pure DEX. This suggests PVP

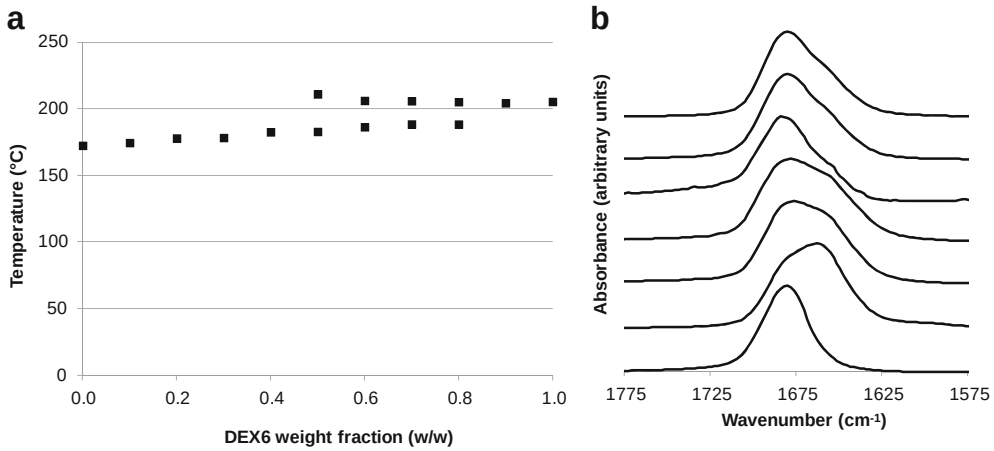

Fig. 3 Representative DSC and FTIR results for DEX6-based systems: (**a**) variation of the T_g as a function of the DEX weight fraction for the DEX6-PVP25 system, and (**b**) changes in the PVP carbonyl stretching peak as a function of the PVP grade for DEX6 systems (normalized and offset). Key: from bottom to top: pure PVP12 (reference), 0.5 DEX (w/w) DEX1-PVP12 (reference), 0.5 DEX (w/w) DEX6-PVP12, 0.5 DEX (w/w) DEX6-PVP17, 0.5 DEX (w/w) DEX6-PVP25, 0.5 DEX (w/w) DEX6-PVP30 and 0.5 DEX (w/w) DEX6-PVP90.

miscibility in DEX is lower than DEX miscibility in PVP. This can be rationalized based on the fact that PVP gains hydrogen bonding interactions, since it does not form hydrogen bonds in the pure state. DEX, on the other hand does form hydrogen bonds with itself and replacing these with hydrogen bonds with PVP probably results in a lower overall extent of hydrogen bonding (28). Thus, the PVP-rich phase will contain more DEX while the DEX-rich phase will contain lower amounts of PVP. FTIR data for the 0.5 (w/w) DEX weight fraction samples mixed with different PVP MW grades are provided in Fig. 3b, together with pure PVP12 and 0.5 (w/w) DEX1-PVP12, as references. Clearly, even the DEX6-PVP12 system shows less hydrogen bonding than the DEX1-PVP12 system. While the carbonyl band of the DEX6-PVP17 blend is similar to that of the blend with PVP12, large additional reductions in the extent of PVP-DEX hydrogen bonding are clearly observed as the MW of PVP increases beyond this point (PVP25, PVP30 and PVP90). A similar reduction in hydrogen bonding with increasing PVP molecular weight can be observed for the 0.2 and 0.8 (w/w) DEX weight fractions (Figure S4 in the Supplementary Material), most clearly for the latter weight fraction.

Intermediate MW Dextran (DEX40) with Different PVP Grades

Upon further increasing the molecular weight of DEX to 40 kDa (DEX40), the miscibility gap of the blends widens as illustrated by Fig. 4a which shows DEX40 with PVP25. Data for the other PVP grades are shown in Figure S5 in the Supplementary Material. While for low molecular weight PVP grades (PVP12 and PVP17), the T_g of the PVP-rich phase still tends to increase considerably with increasing DEX weight fractions, those of higher molecular

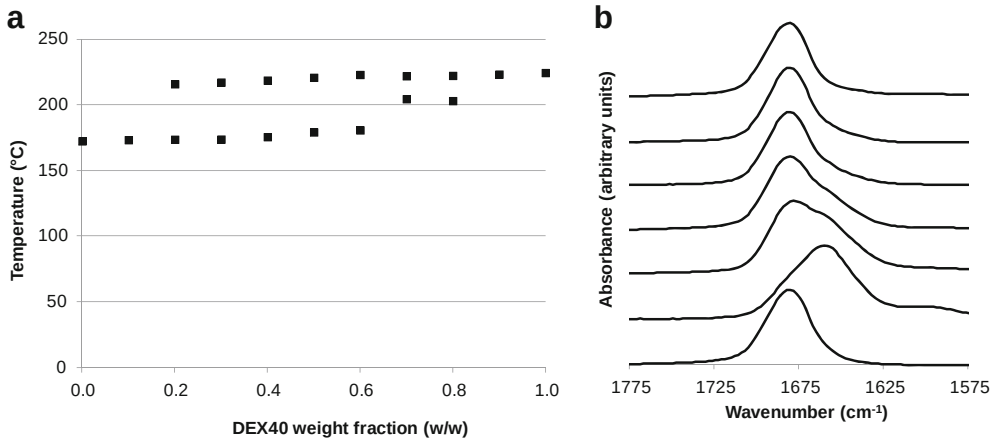

Fig. 4 Representative DSC and FTIR results for DEX40-based systems: (**a**) variation of the T_g as a function of the DEX weight fraction for the DEX40-PVP25 system, and (**b**) changes in the PVP carbonyl stretching peak as a function of the PVP grade for DEX40 systems (normalized and offset). Key: from bottom to top: pure PVP12 (reference), 0.8 DEX (w/w) DEX1-PVP12 (reference), 0.8 DEX (w/w) DEX40-PVP12, 0.8 DEX (w/w) DEX40-PVP17, 0.8 DEX (w/w) DEX40-PVP25, 0.8 DEX (w/w) DEX40-PVP30 and 0.8 DEX (w/w) DEX40-PVP90.

weight PVPs show only small differences compared to the T_g of pure PVP. In contrast, all T_g values of the DEX-rich phases tend to be very similar to that of pure DEX40 and show less dependence on PVP molecular weight. This again suggests the formation of PVP-rich phases with a higher maximum DEX content (that tends to decrease with increasing PVP molecular weight) and DEX-rich phases that are rather limited in terms of the fraction of PVP they can contain. From the FTIR data it is clear that the extent of DEX-PVP hydrogen bonding further decreases. More specifically, only the 0.8 (w/w) DEX weight fractions show a clearly detectable hydrogen bonding shift for PVP12 and PVP17 containing systems which further decreases significantly for higher molecular weight grades of PVP (Fig. 4b). For lower DEX weight fractions, shifts due to hydrogen bonding are much weaker and often hard to identify (Figure S6 in the Supplementary Information). Summarizing, the data obtained on the DEX40 systems show that miscibility and hydrogen bonding tend to further decrease with increasing DEX and/or PVP molecular weights.

High MW Dextran (DEX450) with Different PVP Grades

Finally, DEX450-based blends are considered. From the DSC data (Fig. 5a and Figure S7 in the Supplementary Material), it is clear that, except for the DEX450-PVP12 system, the miscible regions become minimal (for PVP17, PVP25 and PVP30) or even completely disappear (for PVP90). For the DEX450-PVP12 mixtures and the DEX450-PVP17 systems, the T_g of the PVP-rich phase still shows considerable compositional trends. For all other systems and DEX-rich phases, this is not the case. In terms of spectral changes, a further downward trend in DEX-PVP hydrogen bonding can be observed. FTIR data, provided in Fig. 5b for the 0.8 (w/w) DEX systems and in Figure S8 for the 0.2 and 0.5 (w/w) DEX weight fractions, show that, except for the DEX450-PVP12 system, which still shows a certain extent of hydrogen bonding (although greatly reduced compared to DEX1-based systems), little to no hydrogen bonding can be observed in all other systems.

To summarize the results, both blend miscibility as determined from calorimetric T_g measurements and the extent of intermolecular hydrogen bonding between PVP carbonyl groups and DEX hydroxyl groups varies widely, depending on the molecular weight of both polymers. By varying molecular weight, systems can be obtained covering a range from completely miscible and extensively hydrogen bonding to partially miscible with an intermediate level of hydrogen bonding to virtually immiscible with little to no hydrogen bonding.

DISCUSSION

As described above, by varying the molecular weight of the DEX and PVP polymers, a spectrum of miscibility and interpolymer hydrogen bonding can be obtained. The miscibility/immiscibility regions of the different systems, as inferred from the calorimetric T_g have been graphically summarized in Table III. The main observable trend is that the miscibility gap increases with an increase in the MW of both components.

While the DSC results are fairly easily summarized, based on the occurrence of a single T_g or two T_g events, the FTIR spectra are much harder to compare in a quantitative manner. As discussed above, the peak shifts in the carbonyl band of PVP arise from hydrogen bonding with DEX; such peak shifts in carbonyl function of PVP in the presence of a hydrogen bond donor have been extensively

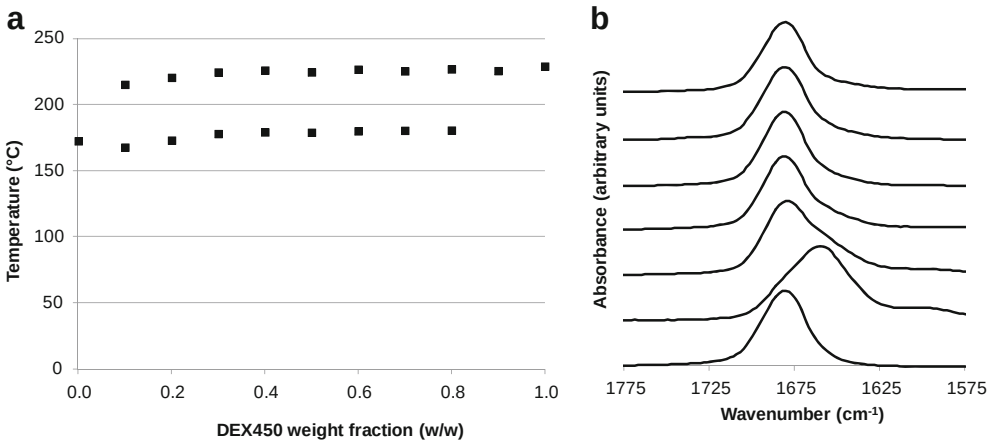

Fig. 5 Representative DSC and FTIR results for DEX450-based systems: (**a**) variation of the T_g as a function of the DEX weight fraction for the DEX450-PVP25 system, and (**b**) changes in the PVP carbonyl stretching peak as a function of the PVP grade for DEX450 systems (normalized and offset). Key: from bottom to top: pure PVP12 (reference), 0.8 DEX (w/w) DEX1-PVP12 (reference), 0.8 DEX (w/w) DEX450-PVP12, 0.8 DEX (w/w) DEX450-PVP17, 0.8 DEX (w/w) DEX450-PVP25, 0.8 DEX (w/w) DEX450-PVP30 and 0.8 DEX (w/w) DEX450-PVP90.

Table III Schematic Overview of the Miscibility Behavior of the DEX-PVP Systems as Derived from DSC Measurements. Key: Miscible Region (*black*), Immiscible Phase Separated Region (*gray*), Actual Measurement (*solid*), Inferred by Considering Neighboring Compositions and Molecular Weight Trends (*shaded*)

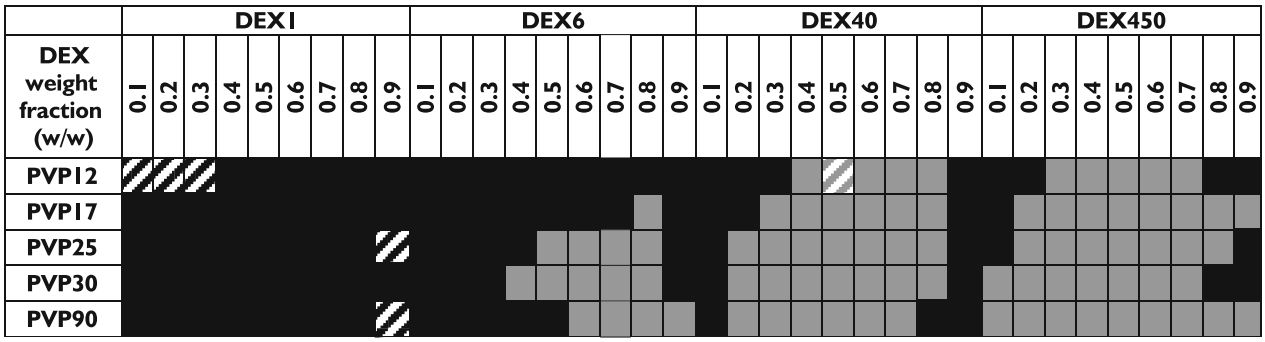

documented (e.g. 28, 30–33). For the DEX1-PVP12 system, it was found that, upon dilution of PVP with DEX, hydrogen bonding increases, reaching a plateau at a DEX weight fraction of 0.8 and 0.9 (w/w), in agreement with previous studies. Based on this observation, it is reasonable to assume that at these compositions, where PVP is miscible with and highly diluted in DEX, the extent of hydrogen bonding of PVP with DEX hydroxyl functions is maximal. As noted earlier, this is not necessary the same as stating that all PVP carbonyl groups are hydrogen bonded at that point, as there is likely to be a fraction of PVP groups that cannot hydrogen bond due to e.g. steric hindrance (34). Bearing this interpretation in mind, we can use this state of maximal PVP hydrogen bonding to enable a more quantitative evaluation of the hydrogen bonding in the different systems. Both the non-hydrogen bonded PVP carbonyl peak and the maximally hydrogen bonded PVP carbonyl peak [taken to be that in the 0.9 (w/w) DEX weight fraction of the DEX1-PVP12 system] are fitted using the peak fitting routine described in the Materials and Methods section. As such, the carbonyl peaks in the spectra of the blends can be expressed in terms of areas of fitted free (A_F) and maximum hydrogen bonded (A_{HB}) carbonyl bands . This enables the extent of hydrogen bonding in the blend (relative to the maximum hydrogen bonding observed) to be determined using Eq. 1 (33):

$$f_{HB} = \frac{\frac{a_F}{a_{HB}} \times A_{HB}}{A_F + \left(\frac{a_F}{a_{HB}} \times A_{HB}\right)} \quad (1)$$

Where f_{HB} is the fraction of hydrogen bonding and a_F/a_{HB} is the ratio of the molar absorption coefficients of the free and hydrogen-bonded carbonyl bands. For the latter, a value of 1.3 was taken from literature (33). Based on the above analysis, it is clear that the f_{HB} values obtained can be interpreted as the number of carbonyl groups that hydrogen bond, relative to the maximum number of carbonyls that can undergo hydrogen bonding (i.e. not necessarily all the carbonyl groups). As such, hydrogen bonding can be assessed in a more quantitative way.

Results for the different systems are shown in Fig. 6. For the DEX1-PVP12 systems (Fig. 6a), hydrogen bonding fraction initially tends to increase rapidly [0.1–0.4 (w/w) DEX]. Subsequently, more moderate increases in hydrogen bonding can be observed [0.5–0.7 (w/w) DEX], followed by the formation of a plateau, where the extent of hydrogen bonding is maximal [0.8–0.9 (w/w) DEX, both f_{HB} values are 1.00]. The overall profile is well described by a quadratic curve ($f_{HB} = -0.00013 \times f_D^2 + 0.02238 \times f_D + 0.02138$; R^2=0.993), note that this equation is just used for fitting purposes and has no physical significance), and the latter curve was included in the other graphs shown in Fig. 6 for comparison purposes. It is apparent from Fig. 6a, that a similar profile of hydrogen bonding is obtained for DEX1 with all PVP MW grades. This result is in good agreement with the DSC data where complete miscibility was observed, independent of the PVP molecular weight.

For the DEX6-based systems (Fig. 6b), it is clear that fraction of hydrogen bonding of the PVP carbonyl groups decreases with increasing PVP MW. At 0.2 weight fraction of DEX, hydrogen bonding in the PVP12 and PVP17 systems (points lie on top of each other) is similar to that in the DEX1-based systems, while for higher PVP grades, the fraction of hydrogen bonded PVP groups tends to decrease when compared with the DEX1-systems (the PVP25, PVP30 and PVP90 points lie on top of each other). At 0.5 DEX weight fractions, a decrease in hydrogen bonding can be noted for all systems (the DEX6-PVP25 system appears to be an outlier since it does not follow the same trends as the other PVP MWs and was characterized by the largest fitting error of all systems evaluated, as can be seen from Table S1). For the 0.8 fractions, all systems show a decrease in hydrogen bonding with larger decreases for higher PVP molecular weights.

Further decreases in hydrogen bonding are observed for the DEX40-based systems (Fig. 6c). For the 0.2 DEX weight

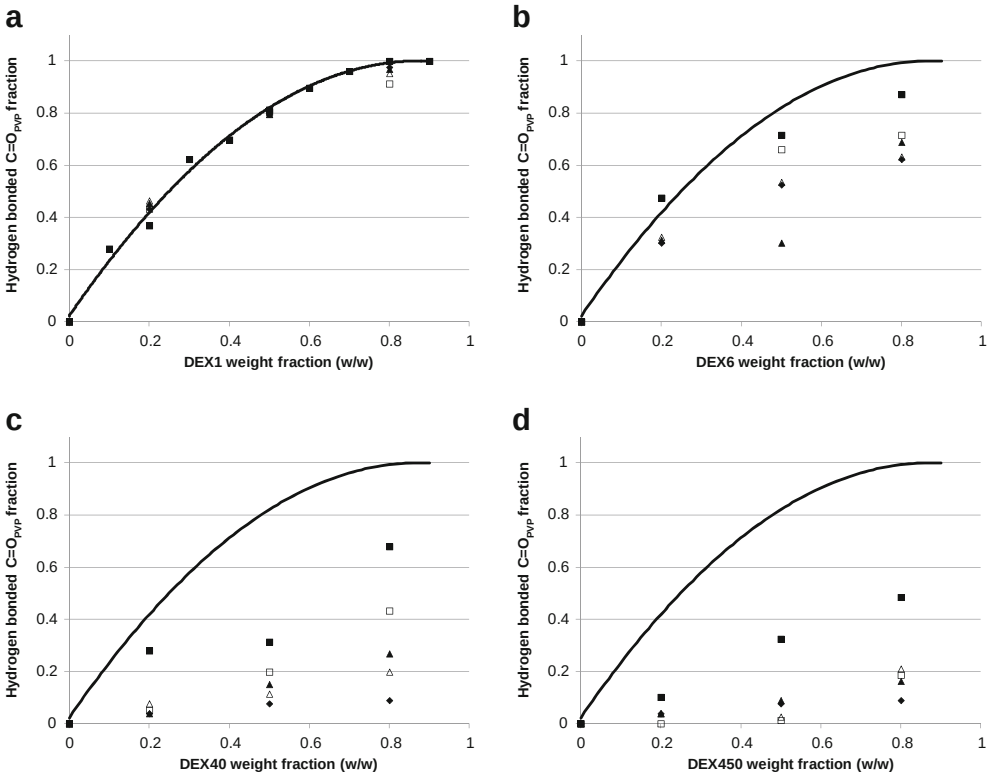

Fig. 6 Fraction of hydrogen bonding calculated by fitting of the carbonyl stretching peak as a function of DEX weight fraction (w/w): (**a**) DEX1 systems, (**b**) DEX6 systems, (**c**) DEX40 systems, and (**d**) DEX450 systems. Key: PVP12 (■), PVP 17 (□), PVP25 (▲), PVP30 (Δ) and PVP90 (♦). The quadratic fitted curve of the PVP12-DEX1 system is included in all graphs for reference.

fractions, PVP12 shows a reasonable extent of hydrogen bonding while hydrogen bonding with all other grades is negligible. The points at 0.5 and 0.8 DEX weight fractions show increases in hydrogen bonding, although overall much reduced compared to that seen in DEX1-based systems. There is a nice trend of decreasing hydrogen bonding for higher PVP grades in these samples.

Finally, DEX450 blends are shown in Fig. 6d. A further reduction in hydrogen bonding can be seen for these blends. Except for the DEX450-PVP12 system, which still shows some extent of hydrogen bonding (although greatly reduced compared to DEX1-based systems), minimal hydrogen bonding is observed in all other systems. Even at large dilutions (0.8 DEX weight fraction), hydrogen bonding is minimal, not exceeding a value of 0.2.

Based on the previous analysis, it is clear that the miscibility behavior of the DEX-PVP model systems studied shows a strong dependence on the molecular weight of both polymers. At this point, it is of interest to consider molecular weight effects on mixing thermodynamics. The free energy of mixing can be described by (Eq. 2):

$$\Delta G_{mix} = \Delta H_{mix} - T\Delta S_{mix} \tag{2}$$

Where ΔG_{mix} is the free energy of mixing, ΔH_{mix} the enthalpy of mixing and ΔS_{mix} the entropy of mixing at the (absolute) mixing temperature T. According to the simplified lattice model (Flory-Huggins theory), the enthalpy of mixing per lattice site is given by (Eq. 3):

$$\Delta H_{mix} = kT\chi\phi_1\phi_2 \tag{3}$$

Where k is the Boltzmann constant, χ the Flory-Huggins interaction parameter (a parameter characterizing the difference of interaction energies in the mixture) and ϕ_1 and ϕ_2 are the volume fraction of the two polymers (35). The entropic contribution to the free energy of mixing per lattice site can be written as Eq. (4):

$$-T\Delta S_{mix} = kT\left[\frac{\phi_1}{N_1}\ln\phi_1 + \frac{\phi_2}{N_2}\ln\phi_2\right] \tag{4}$$

With N_1 and N_2 the number of lattice sites occupied by each polymer molecule (35).

The Flory-Huggins equation serves as a good starting point to rationalize the influence of molecular weight on the observed miscibility behavior seen for the DEX-PVP systems, recognizing that there are a number of limitations to this model (35–37). It is of particular interest to evaluate the influence of MW on the entropy of mixing for the polymers studied herein, since we anticipate that this will vary widely among the different combinations based on Eq. 4. The entropy of mixing is key for the PVP dextran system, since it is anticipated that the enthalpy of mixing between

PVP and DEX is unfavorable. The rationale for this is that the combinatorial entropy is always positive and therefore favorable to mixing, hence if a system shows a miscibility gap, there must be an opposing enthalpy of mixing term. In other words, formation of PVP-DEX interactions occurs at the cost of DEX-DEX (and PVP-PVP) interactions (29) and the unfavorable mixing enthalpy can only be counterbalanced by a favorable enough value for the entropy of mixing if the system is to show miscibility. With respect to the Flory-Huggins parameter, it should be noted that this parameter is not that easily accessible experimentally, but if we assume that it is relatively independent of MW, based on the consideration that chemical composition does not change with MW, then differences in the combinatorial entropy of mixing for the different systems can be directly compared.

Calculations of the entropic contribution to the free energy of mixing (depicted as the free energy of mixing per lattice site with no enthalpic contributions and entropy described by Eq. 4) at 25 °C as a function of the DEX weight fraction are provided in Fig. 7. For both polymers, a density value of 1.2 g/ml was assumed, the PVP monomer was taken as the lattice site, and for polymers where a molecular weight range was provided, the average of that range was used for calculations. For DEX1-based systems (Fig. 7a), results are similar for different PVP MW grades and favorable (more negative) compared to other DEX-grades. The low DEX molecular weight underlies this behavior. This is in line with the complete miscibility and extensive hydrogen bonding observed in these systems. Less negative free energies of mixing and larger differences between PVP12 and higher PVP grades are observed for the DEX6 systems (Fig. 7b), in agreement with the observation that the PVP12 systems were completely miscible, while for higher PVP grades a miscibility gap could be observed. This trend further extends towards the DEX40 and DEX450 systems (Fig. 7c and d, respectively). Again, this is in line with the observation that PVP12 shows higher miscibility and hydrogen bonding compared to higher PVP grades. In addition, it is worth noting that for the DEX450-PVP90

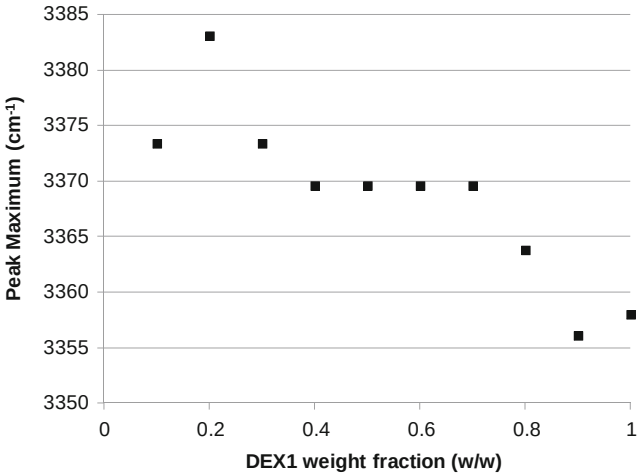

Fig. 8 Peak maxima of the DEX OH stretching vibration as a function of the DEX weight fraction in the DEX1-PVP12 system.

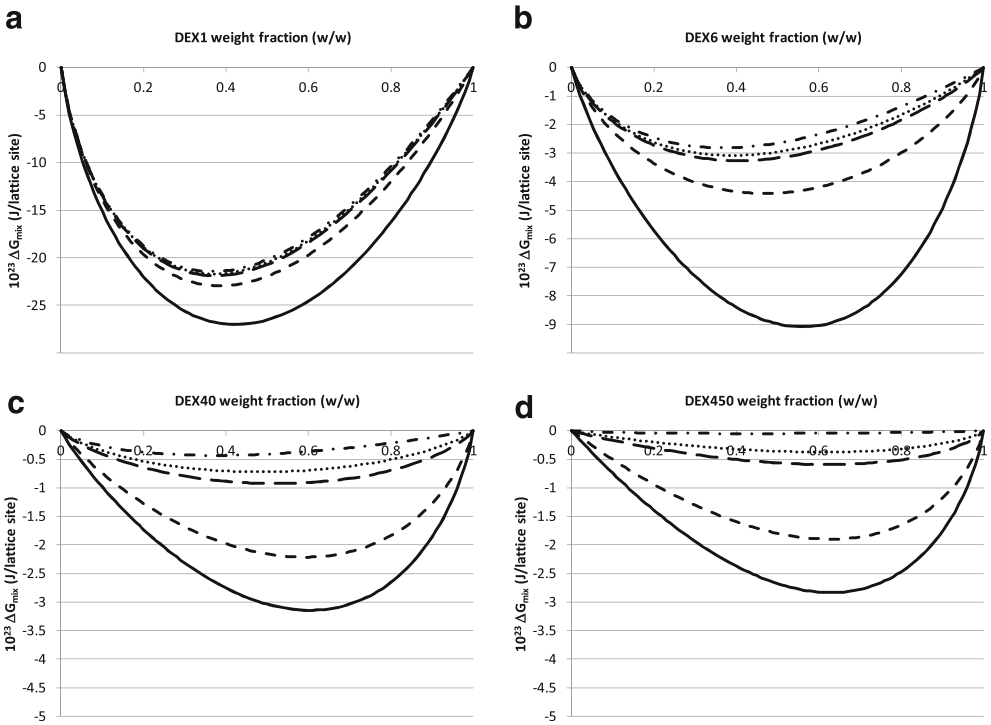

Fig. 7 Entropic part of the free energy of mixing per lattice site as a function of DEX weight fraction (w/w): (**a**) DEX1 systems, (**b**) DEX6 systems, (**c**) DEX40 systems, and (**d**) DEX450 systems. Key: PVP12 (*solid*), PVP 17 (*short dash*), PVP25 (*long dash*), PVP30 (*dotted*) and PVP90 (*dash-dot*).

system, the entropic contribution to the free energy of mixing becomes virtually zero. Finally, given the phase separation observed in many of the systems, it is clear that the enthalpic part of the free energy of mixing has to be positive, resulting in phase separation in systems where the entropy of mixing is not sufficiently large to counterbalance this term. In other words, DEX-DEX interactions can be considered energetically more favorable than DEX-PVP interactions, which may stem from the DEX-DEX hydrogen bond being stronger and/or more numerous than the DEX-PVP hydrogen bonds. Support for this is provided from IR data that show a blue shift in the dextran OH vibration peak maximum with increasing PVP amount (lower DEX weight fraction) for the fully miscible DEX1-PVP12 system, indicating an overall decrease in the extent of DEX-DEX hydrogen bonding with increasing DEX-PVP hydrogen bonding (Fig. 8).

CONCLUSIONS

Depending of the molecular weights used to prepare DEX-PVP blends, miscibility can vary from completely miscible to virtually immiscible. The higher the combined polymer molecular weights, the lower the miscibility of the resultant blends. Lower miscibility also coincides with a lower extent of inter-polymer hydrogen bonding between the hydroxyl groups of DEX and the carbonyl groups of PVP. Upon further consideration of the thermodynamics of mixing it was surmised that (i) the enthalpy of mixing is positive for these systems (ii) the entropy of mixing rapidly becomes less favorable with increasing molecular weights and therefore cannot offset the unfavorable enthalpy of mixing. Given the fact that, depending on the molecular weights of the polymers, chemically similar systems with tunable miscibility characteristics can be obtained and have been characterized in depth, DEX-PVP systems can be considered as excellent model systems for the evaluation of analytical techniques aiming at characterizing miscibility behavior.

ACKNOWLEDGMENTS & DISCLOSURES

The authors thank the National Science Foundation Engineering Research Center for Structured Organic Particulate Systems (NSF ERC-SOPS)(EEC-0540855) for financial support. Elisabeth M. Topp, Ph.D. and Andreas M. Sophocleous, Ph.D. are thanked for providing access to the lyophilizer and help with freeze-drying experiments, respectively. BVE is a Postdoctoral Researcher of the 'Fonds voor Wetenschappelijk Onderzoek', Flanders, Belgium.

REFERENCES

1. Leuner C, Dressman J. Improving drug solubility for oral delivery using solid dispersions. Eur J Pharm Biopharm. 2000;50(1):47–60.
2. Van Eerdenbrugh B, Taylor LS. Small scale screening to determine the ability of different polymers to inhibit drug crystallization upon rapid solvent evaporation. Mol Pharmaceutics. 2010;7(4):1328–37.
3. Van Eerdenbrugh B, Taylor LS. An ab initio polymer selection methodology to prevent crystallization in amorphous solid dispersions by application of crystal engineering principles. CrystEngComm. 2011;13(20):6171–78.
4. Baird JA, Taylor LS. Evaluation of amorphous solid dispersion properties using thermal analysis techniques. Adv Drug Delivery Rev. doi:10.1016/j.addr.2011.07.009.
5. Randolph TW. Phase separation of excipients during lyophilization: effects on protein stability. J Pharm Sci. 1997;86(1):1198–203.
6. Utracki LA. Glass transition temperature in polymer blends. Adv Polym Technol. 1985;5:33–9.
7. Newman A, Engers D, Bates S, Ivanisevic I, Kelly RC, Zografi G. Characterization of amorphous API:polymer mixtures using X-ray powder diffraction. J Pharm Sci. 2008;97:4840–56.
8. Rumondor ACF, Marsac PJ, Stanford LA, Taylor LS. Phase behavior of poly(vinylpyrrolidone) containing amorphous solid dispersions in the presence of moisture. Mol Pharmaceutics. 2009;6(5):1492–505.
9. Marsac PJ, Rumondor ACF, Nivens DE, Kestur US, Stanciu L, Taylor LS. Effect of temperature and moisture on the miscibility of amorphous dispersions of felodipine and poly(vinyl pyrrolidone). J Pharm Sci. 2010;99(1):169–85.
10. Rumondor ACF, Ivanisevic I, Bates S, Alonzo DE, Taylor LS. Evaluation of drug-polymer miscibility in amorphous solid dispersion systems. Pharm Res. 2009;26(11):2523–34.
11. Ivanisevic I, Bates S, Chen P. Novel methods for the assessment of miscibility of amorphous drug-polymer dispersions. J Pharm Sci. 2009;98(9):3373–86.
12. Padilla AM, Ivanisevic I, Yang YL, Engers D, Bogner RH, Pikal MJ. The study of phase separation in amorphous freeze-dried systems. part I: Raman mapping and computational analysis of XRPD data in model polymer systems. J Pharm Sci. 2011;100(1):206–22.
13. Qi S, Belton P, Nollenberger K, Clayden N, Reading M, Craig DQM. Characterisation and prediction of phase separation in hot-melt extruded solid dispersions: a thermal, microscopic and NMR relaxometry study. Pharm Res. 2010;27(9):1869–83.
14. Aso Y, Yoshioka S, Miyazaki T, Kawanishi T, Tanaka K, Kitamura S, Takakura A, Hayashi T, Muranushi N. Miscibility of nifedipine and hydrophilic polymers as measured by H-1-NMR spin-lattice relaxation. Chem Pharm Bull. 2007;55(8):1227–31.
15. Pham TN, Watson SA, Edwards AJ, Chavda M, Clawson JS, Strohmeier M, Vogt FG. Analysis of amorphous solid dispersions using 2D solid-state NMR and ^{1}H T_1 relaxation measurements. Mol Pharmaceutics. 2010;7(5):1667–91.
16. Lauer ME, Grassmann O, Siam M, Tardio J, Jacob L, Page S, Kindt JH, Engel A, Alsenz J. Atomic force microscopy-based screening of drug-excipient miscibility and stability of solid dispersions. Pharm Res. 2011;28(3):572–84.
17. Padilla AM, Pikal MJ. The study of phase separation in amorphous freeze-dried systems, part 2: investigation of Raman mapping as a tool for studying amorphous phase separation in freeze-dried protein formulations. J Pharm Sci. 2011;100(4):1467–74.
18. Padilla AM, Chou SG, Luthra S, Pikal MJ. The study of amorphous phase separation in a model polymer phase-separating system using Raman microscopy and a low-temperature stage:

effect of cooling rate and nucleation temperature. J Pharm Sci. 2011;100(4):1362–76.
19. Qi S, Belton P, Nollenberger K, Gryckze A, Craig DQM. Compositional analysis of low quantities of phase separation in hot-melt-extruded solid dispersions: a combined atomic force microscopy, photothermal Fourier-transform infrared microspectroscopy, and localised thermal analysis approach. Pharm Res. 2011;28(9):2311–26.
20. Six K, Murphy J, Weuts I, Craig DQM, Verreck G, Peeters J, Brewster M, Van den Mooter G. Identification of phase separation in solid dispersions of itraconazole and Eudragit® E100 using microthermal analysis. Pharm Res. 2003;20(1):135–8.
21. Galop M. Study of pharmaceutical solid dispersions by microthermal analysis. Pharm Res. 2005;22(2):293–302.
22. Zhang J, Bunker M, Parker A, Madden-Smith CE, Patel N, Roberts CJ. The stability of solid dispersions of felodipine in polyvinylpyrrolidone characterized by nanothermal analysis. Int J Pharm. 2011;414(1–2):210–7.
23. Van Eerdenbrugh B, Taylor LS. Application of mid-IR spectroscopy for the characterization of pharmaceutical systems. Int J Pharm. 2011;417(1–2):3–16.
24. Van Eerdenbrugh B, Lo M, Kjoller K, Marcott C, Taylor LS. Nanoscale Mid-Infrared Imaging of Phase Separation in a Drug-Polymer Blend. J Pharm Sci. Submitted.
25. Izutsu K, Heller MC, Randolph TW, Carpenter JF. Effect of salts and sugars on phase separation of polyvinylpyrrolidone-dextran solutions induced by freeze-concentration. J Chem Soc, Faraday Trans. 1998;94(3):411–7.
26. Izutsu K, Aoyagi N, Kojima S. Effect of polymer size and cosolutes on phase separation of poly(vinylpyrrolidone) (PVP) and dextran in frozen solutions. 2005;94(4):709–717.
27. Izutsu K, Fujii K, Katori C, Yomota C, Kawanishi T, Yoshihashi Y, Yonemochi E, Terada K. Effects of solute miscibility on the micro- and macroscopic structural integrity of freeze-dried solids. J Pharm Sci. 2010;99(11):4710–9.
28. Shamblin SL, Taylor LS, Zografi G. Mixing behavior of colyophilized binary systems. J Pharm Sci. 1998;87(6):694–701.
29. Taylor LS, Zografi G. Sugar-polymer hydrogen bonding interactions in lyophilized amorphous mixtures. J Pharm Sci. 1998;87(2):1615–21.
30. Patterson D, Robarb A. Thermodynamics of polymer mixing. Macromolecules. 1978;11(4):690–5.
31. Janarthanan V, Thyagarajan G. Miscibility studies in blends of poly(N-vinyl pyrrolidone) and poly(methyl methacrylate) with epoxy-resin—a comparison. Polymer. 1992;33(17):3593–7.
32. Zhu KJ, Liquin W, Ji W, Shilin Y. Study of the miscibility of poly(N-vinyl-2-pyrrolidone) with polystyrene[styrene-co-(4-hydroxystyrene)]. Macromol Chem Phys. 1994;195(6):1965–72.
33. Ahn SB, Jeong HM. Phase behavior and hydrogen bonding in poly (ethylene-co-vinyl alcohol) poly(N-vinyl-2-pyrrolidone) blends. Korea Polym J. 1998;6(5):389–95.
34. Garton A. Some Observations on Kinetic and Steric Limitations to Specific Interactions in Miscible Polymer Blends. Polym Eng Sci. 1984;24(2):112–6.
35. Rubinstein M, Colby RH. Polymer Physics. New York: Oxford University Press Inc.; 2003.
36. Young RJ, Lovell PA. Introduction to polymers. Cheltenham: Nelson Thornes; 1991.
37. Flory PJ. Principles of polymer chemistry. Ithaca: Cornell University Press; 1953.